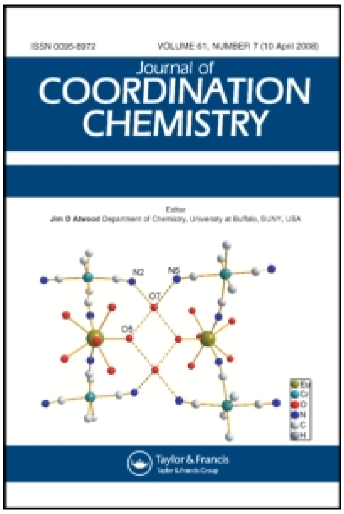

Journal of Coordination Chemistry
Publication details, including instructions for authors and subscription information:
http://www.informaworld.com/smpp/title~content=t713455674

Structures of Mn(II) complexes of bis(2-pyridylmethyl)amine (bpa) and (2-pyridylmethyl)(6-methyl-2-pyridylmethyl)amine (Mebpa): geometric isomerism in the solid state

Yilma Gultneh[a]; Bijan Ahvazi[a]; Yohannes T. Tesema[a]; Teshome B. Yisgedu[a]; Ray J. Butcher[a]
[a] Department of Chemistry, Howard University, Washington, DC 20059

To cite this Article Gultneh, Yilma , Ahvazi, Bijan , Tesema, Yohannes T. , Yisgedu, Teshome B. and Butcher, Ray J.(2006) 'Structures of Mn(II) complexes of bis(2-pyridylmethyl)amine (bpa) and (2-pyridylmethyl)(6-methyl-2-pyridylmethyl)amine (Mebpa): geometric isomerism in the solid state', Journal of Coordination Chemistry, 59: 16, 1835 — 1846

To link to this Article: DOI: 10.1080/00958970600644609

URL: http://dx.doi.org/10.1080/00958970600644609

Journal of Coordination Chemistry
Vol. 59, No. 16, 10 November 2006, 1835–1846

Taylor & Francis
Taylor & Francis Group

Structures of Mn(II) complexes of bis(2-pyridylmethyl)amine (bpa) and (2-pyridylmethyl)(6-methyl-2-pyridylmethyl)amine (Mebpa): geometric isomerism in the solid state

YILMA GULTNEH*, BIJAN AHVAZI†, YOHANNES T. TESEMA‡,
TESHOME B. YISGEDU§ and RAY J. BUTCHER

Department of Chemistry, Howard University,
Washington, DC 20059

(*Received 30 March 2005; in final form 27 October 2005*)

The crystal structures of $[Mn(bpa)_2](ClO_4)_2$ (**1**), [bpa = bis(2-pyridylmethyl)amine], and $Mn(6\text{-}Mebpa)_2(ClO_4)_2$ (**2**), [6-Mebpa = (6-methyl-2-pyridylmethyl)(2-pyridylmethyl)amine] have been determined. In **1**, two facial $[Mn(bpa)_2]^{2+}$ isomers are observed in the same unit cell, one with C_i (**1a**) and the other with C_2 (**1b**) symmetries. In **2**, only the isomer with C_2 symmetry is observed. The structure of $[Mn(bpa)_2]^{2+}$ with only C_2 symmetry has been reported previously (*Inorg. Chem.*, **31**, 4611 (1992)). The bond length order $Mn\text{–}N_{amine} > Mn\text{–}N_{pyridyl}$, observed in the C_2 and the C_i isomers in the crystals of **1**, is the reverse of the order observed in the structure of $[Mn(bpa)_2](ClO_4)_2$ which contains only the C_2 isomer in the unit cell. The structure of **2** in which only the C_2 isomer is found, also shows the bond length order $Mn\text{–}N_{pyridyl} > Mn\text{–}N_{amine}$. In cyclic voltammetric experiments in acetonitrile solutions, **1** and **2** show irreversible anodic peaks at $E_p = 1.60$ and $1.90\,V$ respectively, (*vs.* Ag/AgCl), assigned to the oxidation of Mn(II) to Mn(III). The substantially higher oxidation potential of **2** is attributable to a higher rearrangement energy in complex **2** due to the steric effect of the methyl substituent.

Keywords: Manganese; Bis(2-pyridylmethyl)amine; 2-Pyridylmethlyl(6-methyl-2-pyridylmethyl)amine; Isomerism

1. Introduction

Isomerism of six-coordinate metal complexes ML_2, where L is a tridentate ligand with two identical chelating arms about a central secondary amine donor, has been shown in the Zn(II) complex [1]. Common examples of this class of ligands include

---

*Corresponding author. Email: ygultneh@howard.edu
†Current address: Office of Science and Technology, X-ray Crystallography Facility NIH, Bethesda, MD 20892-1820.
‡Current address: Chemistry Dept., Duke University, Durham, NC 27708.
§Current address: Chemistry Dept., The Ohio State University, Columbus, Ohio 43210.

Journal of Coordination Chemistry
ISSN 0095-8972 print/ISSN 1029-0389 online © 2006 Taylor & Francis
DOI: 10.1080/00958970600644609

bis(2-pyridylmethyl)amine (bpa) (a, see structure below), (2-pyridylmethyl)(6-methyl-2-pyridylmethyl)amine (Mebpa) (b) and bis(benzimidazol-2′-ylmethyl)amine (bba). Of the meridional and facial geometric isomers possible in such complexes, the facial

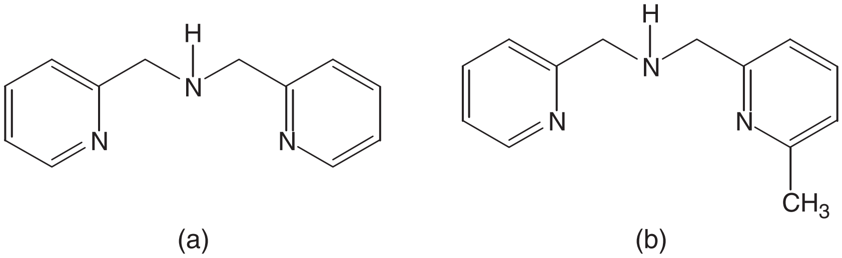

isomer could have either a two-fold axis (C_2) or a center of symmetry (C_i) figure 1), the former of which could exist as an enantiomeric pair.

In the six-coordinate complexes $[Cu(bpa)_2](BF_4)_2$ [2], $[Cu(bba)_2](ClO_4)_2 \cdot 2H_2O$ [3], $[Fe(bpa)_2](BF_4)_2$ [4], $[Zn(bpa)_2](ClO_4)_2$, $[Cd(bpa)_2](ClO_4)_2$, and $[Mn(bpa)_2](ClO_4)_2$ [1], only *cis*-facial coordination has been observed. However in some pentacoordinate complexes such as $[Cu(bpa)_2](BF_4)_2$ [2], $[Cu(B\text{-}MIMA)(OAc)](ClO_4)$ [5] (B-MIMA = bis(2-(1-methyl)imidazolyl)methyl)amine) and $[Zn(bpa)(H_2O)_2](ClO_4)_2$ [6] meridional coordination has been found. Glerup *et al.* reported [1] the structures of *facial* $M(II)(bpa)_2(ClO_4)_2$ (M = Cd, Mn, and Zn) in which Cd and Mn are coordinated with C_2 symmetry whereas Zn^{2+} ions are observed to coordinate with both C_2 and C_i symmetries in the same crystal lattice. In contrast, Zn^{2+} is found only in C_i symmetry in the complex $[Zn(bpa)_2]Cl_2 \cdot 6H_2O$. We report here the crystal structures of *facial* $[Mn(bpa)_2](ClO_4)_2$ (**1**) in which the Mn(II) ions are found coordinated with both C_i and the C_2 symmetry in the same unit cell, and the structure $[Mn(6\text{-}methyl\text{-}bpa)_2](ClO_4)_2$ (**2**) in which Mn(II) is observed with C_2 symmetry only.

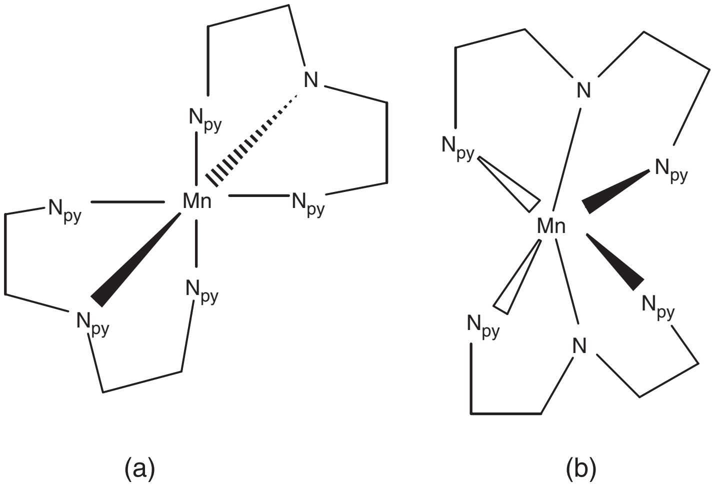

Figure 1. Skeletal drawing of the geometric isomeric forms of $[Mn(bpa)_2]^{2+}$ with C_i (a) and C_2 (b) symmetry (N_{py} = pyridyl N).

2. Experimental

2.1. *Materials and methods*

All chemicals and solvents used were reagent grade. Solvents were dried and distilled under nitrogen. Ether was dried and distilled over Na/benzophenone, acetonitrile was refluxed over CaH_2 overnight, filtered and further passed through an activated alumina column and methanol was dried over $Mg(OCH_3)_2$ under nitrogen. Molar conductivity studies in acetonitrile solution were performed on a Fisher Accumet 50 pH meter/conductivity bridge using YSI conductance cell (0.10 cm) by the Onsanger plot method. Elemental analyses on the three complexes were done by Desert Analytics, Tucson, Arizona and MHW laboratories, Phoenix, AZ. Room temperature magnetic susceptibility measurements were done using the Johnson-Matthey susceptibility balance with $Hg(Co(CN)_4)$ as standard and magnetic moments calculated with diamagnetic corrections. Cyclic voltammetric experiments were performed using a BAS100 electrochemical work station, BAS glassy carbon microlectrode, Ag/AgCl reference and Pt counter electrode. Typically acetonitrile solutions that are 10 mM in the Mn(II) complexes and 0.10 M in Et_4NPF_6 were used. Infrared experiments were done in nujol mull on a Perkin-Elmer FT IR spectrometer (polystyrene reference). ^1H and ^{13}C NMR spectra were taken on a GE 300, 300 MHz spectrometer with TMS as internal reference.

2.2. *Synthesis of ligands*

2.2.1. Synthesis of bis(2-pyridylmethyl)amine (bpa). This ligand was prepared by a literature method [7] and purified by fractional distillation under reduced pressure (b.p. 147–149°C at 0.10 mm Hg).

2.2.2. Synthesis of 6-methyl-2-bromomethylpyridine. (Bromolutidine): 2,6-lutidine (10.0 g (93.3 mmol), was dissolved in 150 mL of carbon tetrachloride and to this was added 16.6 g (93.3 mmol) NBS and 0.25 g benzoylperoxide. The mixture was refluxed for 2.5 h and another portion of 0.1 g benzoyl peroxide was added and refluxed for another 1 h. The solution cooled overnight. The succinimide precipitate was filtered off and the solvent was removed from the filtrate by rotary-evaporation yielding a light brown oil. This was distilled under vacuum to give 7.2 g (40%) of pale pink oil which solidified upon standing in the refrigerator. ^1H NMR ($CDCl_3$): 7.44 (t, 3-H, 1H), 7.11 (d, 3-H, 1H), 7.02 (d, 5-H, 1H), 4.40 (s, CH_2–Br, 2H), 2.42 (s, CH_3, 3H); C-13 NMR ($CDCl_3$): 157.93 (6-C), 155.64 (2-C), 136.84 (4-C), 122.24 (5-C), 120.08 (3-C), 33.82 (7-C), 24.00 (1-C); GC/MS ($R_t = 6.2$ min) 187/185 (M^+, 12.5), 106 (M–Br, 1000), 79 (40.6), 77 (M–CH_2Br, CH_3; 18.8), 63 (M–CH_2Br, CH_3, CH_2; 7.8), 39 (19), 28 ($CH_2CH_2^+$, 7).

2.2.3. Synthesis of 2-pyridylmethyl-(6-methyl-2-pyridylmethyl)amine (Mebpa). This ligand was prepared by the reaction of 2-pyridylmethylamine and bromolutidine by a procedure similar to that of bpa. To a stirred 10.0 g (92.5 mmol) of 2-aminomethylpyridine cooled to 0°C was added 4.3 g (23.1 mmol) bromolutidine, dropwise, and the mixture was stirred at 0°C for 3 hours followed by room temperature overnight.

Water (10 mL) was added, the pH was adjusted to about 10 by adding dilute aqueous NaOH dropwise and the mixture stirred overnight. The resulting thick brown oily layer was extracted with methylene chloride (3 × 50 mL). The extracts were combined and dried over anhydrous magnesium sulfate followed by filtration. After removing the solvent on a rotary evaporator under reduced pressure, the product was isolated as a pale yellow oil by vacuum distillation (b.p. 155°C at 0.1 mm Hg; yield 13.5 g: 72%). ^{1}H NMR: ($CDCl_3$, δ (ppm vs TMS = 0)) 8.47 (d, 1H), 7.53 (t, 1H), 7.43 (t, H-7, 1H), 7.27 (d, 2H), 7.07 (m, 2H), 6.90 (d, 1H), 3.91 (s, 2H), 3.88 (s, 2H), 2.45 (s, 3H), 2.3 (s, 1H).

2.2.4. Synthesis of the complex $[Mn(bpa)_2](ClO_4)_2$ (1). A degassed solution of 1.99 g (10 mmol) of the ligand in methanol (25 mL) was added to a degassed solution of 1.80 g (5.0 mmol) $Mn(ClO_4)_2 \cdot 6H_2O$ and stirred overnight under argon. The starting yellow solution turned to light brown and produced a brownish precipitate, which was filtered off, washed first with a 1 : 1 mixture of methanol and then with ether and dried under vacuum. Crystals suitable for X-ray diffraction were obtained by recrystallization from nitromethane/ether mixture (yield: 2.7 g, 85%). Elemental analysis: Calcd for $[Mn(bpa)_2](ClO_4)_2$ ($Mn(C_{12}H_{13}N_3)_2Cl_2O_4$): C, 44.19%; N, 12.88%; H, 4.02. Found, C, 44.29%; N, 12.65%; H, 3.94%. The molar conductance in acetonitrile solution was shown to be in the range for 2 : 1 cation-to-anion charge ratio consistent with the formulation $[Mn(II)(bpa)_2]^{2+}$ $(ClO_4^-)_2$. In acetonitrile solution three absorption peaks at (λ_{max} (nm) ε (M^{-1}–cm^{-1})) 236 (815), 262 (910) and 280 (835) were observed, all intra-ligand transitions. The IR spectrum in CH_3CN showed prominent peaks at (cm^{-1}) 3263 (ν(N–H)), 1603 (ν(pyridyl)), and 1098 ($\nu(ClO_4^-)$).

2.2.5. Synthesis of $[Mn(6\text{-}Mebpa)_2](ClO_4)_2$ (2). This complex was synthesized and crystallized by the same procedure as the analogous complex **1** above. Crystals for X-ray crystallography were obtained from acetonitrile/ether solution. Elemental analysis: Calcd (%) for $Mn(C_{13}H_{17}N_3)_2(Cl_2O_8)$: C, 45.9; H, 4.41; N, 12.35. Found (%): C, 46.06, H, 4.40, N, 12.22.

2.3. *X-ray diffraction crystal structure determination for complexes 1 and 2*

The crystal was mounted in a random orientation on the end of a glass fiber using 5 min cement and transferred to a goniometer. Preliminary crystal parameters and reflections data were obtained at room temperature and processed by standard methods [8, 9] on a Siemens P4S four circle X-ray diffractometer using a graphite monochromator on the incident beam and a Siemens 486-based PC [10]. Crystal data collection and refinement data are given in table 1. The space group was unambiguously determined from a statistical examination of the intensities of the collected data set. Corrections for decay, absorption and extinction were applied as noted in table 1. Data were collected to the limits of availability. All structures were solved by direct methods [11] as implemented in the SHELXTLPC system [10] of computer programs. The structures were refined to convergence by full-matrix least-squares methods. All hydrogen atoms were found and their positional parameters refined. Atomic scattering factors used were those from the International tables for X-ray crystallography [12].

3. Results and discussion

3.1. *Crystallographic structures*

Tables 2 and 3 show the coordination bond lengths and angles in complexes **1** and **2**, respectively.

3.1.1. Structure of [Mn(bpa)$_2$](ClO$_4$)$_2$ (1). Figure 2(a) and (b) show the ORTEP drawings of the two coordination symmetries of Mn(II) ions, C_i 1a and C_2 1b in **1**. In each isomer Mn(II) is coordinated by six N donor groups from two bpa ligand

Table 1. Summary of crystal data and refinement for structures of **1** and **2**.

	$[Mn(bpa)_2]^{2+}$ (**1**)	$[Mn(6\text{-}Me\text{-}bpa)_2]^{2+}$ (**2**)
Empirical formula	$C_{24}H_{26}Cl_2MnN_6O_8$	$C_{26}H_{30}Cl_2MnN_6O_8$
Formula weight	652.35	680.4
Temperature (K)	293(2)	293(2)
Wavelength (Å)	0.71073	0.71073
Crystal system	Monoclinic	Orthorhombic
Space group	$C2/c$	$Pna2_1$
a (Å)	23.978(3)	19.700(5)
b (Å)	9.0815(13)	8.4036(18)
c (Å)	26.183(4)	18.307(3)
β (°)	91.179(9)	90
Volume (Å^3)	5700.1(14)	3030.8(11)
Z	8	4
D_{Calcd} (Mg m^{-3})	1.520	1.491
Absorption coefficient (mm^{-1})	0.708	0.669
θ range for data collection (°)	2.52 to 27.50	2.35 to 24.00
Reflection collected	6038	2468
Independent reflections	5909	2468
Final R indices $[I > 2\sigma(I)]$	0.0528	0.0844
R indices (all data)	0.1010	0.10(10)

Table 2. Selected bond lengths and bond angles in the two isomeric cations (**1a** and **1b**) in the structure of complex **1**.

	1a		**1b**
Mn(1)–N(1)	2.270(3)	Mn(2)–N(2)	2.341(3)
Mn(1)–N(1)#1	2.270(3)	Mn(2)–N(2)#2	2.341(3)
Mn(1)–N(11A)	2.238(3)	Mn(2)–N(21A)	2.222(3)
Mn(1)–N(11A)#1	2.238(3)	Mn(2)–N(21A)#2	2.222(3)
Mn(1)–N(11B)	2.228(3)	Mn(2)–N(21B)	2.252(3)
Mn(1)–N(11B)#1	2.228(3)	Mn(2)–N(21B)#2	2.252(3)
N(1)–Mn(1)–N(1)#1	180.0	N(2)–Mn(2)–N(2)#2	133.7(2)
N(11A)–Mn(1)–N(11A)#1	180.0	N(21A)–Mn(2)–N(21A)#2	132.8(2)
N(11B)–Mn(1)–N(11B)#1	180.0	N(21B)–Mn(2)–N(21B)#2	86.8(2)
N(11A)–Mn(1)–N(11B)	86.22(11)	N(21A)–Mn(2)–N(21B)	117.87(12)
N(11A)–Mn(1)–N(1)	76.78(12)	N(21A)–Mn(2)–N(2)	72.43(12)
N(11B)–Mn(1)–N(1)	77.15	N(21B)–Mn(2)–N(2)	73.64(12)
N(11B)–Mn(1)–N(11A)#1	93.78(11)	N(21B)–Mn(2)–N(21A)#2	96.58(11)
N(11B)#1–Mn(1)–N(1)	102.86(12)	N(21B)#2–Mn(2)–N(2)	148.56(13)
N(11A)–Mn(1)–N(1)#1	103.22(12)	N(21A)–Mn(2)–N(2)#2	89.22(12)

Table 3. Selected bond lengths (Å) and angles (°) in **2**.

Mn–N(1A)	2.303
Mn–N(1B)	2.288(16)
Mn–N2(A)	2.274(17)
Mn–N2(B)	2.327(16)
Mn–N(3A)	2.319(13)
Mn–N(3B)	2.255(14)
N(1A)–Mn–N(2A)	71.9(7)
N(1B)–Mn–N(2B)	71.9(7)
N(2A)–Mn–N(3A)	73.5(5)
N(2B)–Mn–N(3B)	72.8(5)
N(1A)–Mn–N(3A)	124.7(5)
N(2A)–Mn–N(2B)	139.6(4)
N(2A)–Mn–N(1B)	92.5(6)
N(1A)–Mn–N(2B)	89.3(6)
N(2A)–Mn–N(3B)	140.8(6)
N(3A)–Mn–N(2B)	142.3(5)
N(1A)–Mn–N(1B)	129.3(4)
N(3A)–Mn–N(3B)	88.6(4)
N(1B)–Mn–N(3A)	93.6(5)

molecules in distorted octahedral geometry. The coordination in the C_i isomer is distorted from octahedral geometry as shown by the less than 90° chelate N_{amine}–Mn(1)–$N_{pyridyl}$ angles and interligand *cis* angles greater than 90°. The interligand N_{amine}–Mn(1)–$N_{pyridyl}$ angles (103.22(12)°, 102.86(12)°) are greater than the $N_{pyridyl}$–Mn(1)–$N_{pyridyl}$) angles (93.78(11)°). In the C_2 isomer, the N_{amine}–Mn(2)–$N_{pyridyl}$ chelate angles are less than 90°, whereas the intraligand $N_{pyridyl}$–Mn(2)–$N_{pyridyl}$ angles increase to 117.87(12)°. The N_{amine}–Mn(2)–N_{amine} angle is reduced to 133.7(2)° from 180° in the C_i isomer. Of the two N_{amine}–Mn(2)–$N_{pyridyl}$ interligand angles, one is reduced to 89.23(12)° and the other expanded to 148.56(13)°. The interligand $N_{pyridyl}$–Mn(2)–$N_{pyridyl}$ angles are 132.8(2), 96.58(11) and 86.8(2)°. In this crystalline form of $[Mn(bpa)_2]^{2+}$, while the Mn–N_{amine} bonds are significantly longer than the Mn–$N_{pyridyl}$ bonds in both isomers, the difference is greater in the C_2 isomer (about 0.1 Å) than in the C_i isomer (0.04 Å).

The Mn–N_{amine} bonds in the C_2 isomer are longer (2.341(4) Å) than in the C_i isomer (2.270(3) Å) whereas the Mn–$N_{pyridyl}$ bonds are very nearly the same (average 2.235 ± 0.002 Å) within an isomer and from one isomer to the other. The significant difference between the two isomers therefore is the lengthening of the Mn–N_{amine} bond in the C_2 isomer along with the coordination rearrangements which result in increased $N_{pyridyl}$–Mn(2)–$N_{pyridyl}$ angles, at the expense of the N_{amine}–Mn(2)–N_{amine} bond angle, which relieves steric crowding of the bulky pyridyl groups. Thus there seems to be a balance between longer Mn–N_{amine} and increased angles of bulky groups (C_2) or shorter Mn–N_{amine} with smaller angle between bulky groups (C_i). In the present case, it appears that the structure achieves stability from alternating the two isomers in the packing.

The observed bond length order Mn–N_{amine} > Mn–$N_{pyridyl}$ in both isomers in **1**, is the reverse of the order observed in the structure of another crystalline form of $[Mn(bpa)_2](ClO_4)_2$ that shows only the C_2 isomer [1]. The bond length order Mn–$N_{pyridyl}$ > Mn–N_{amine} is also observed in the structure of $[Mn(Mebpa)_2]^{2+}$ which shows only the C_2 isomer in the crystals (see below). The zinc complex, $[Zn(bpa)_2]^{2+}$ is known to crystallize in the same two forms C_i and C_2, as in **1** and the same relationships

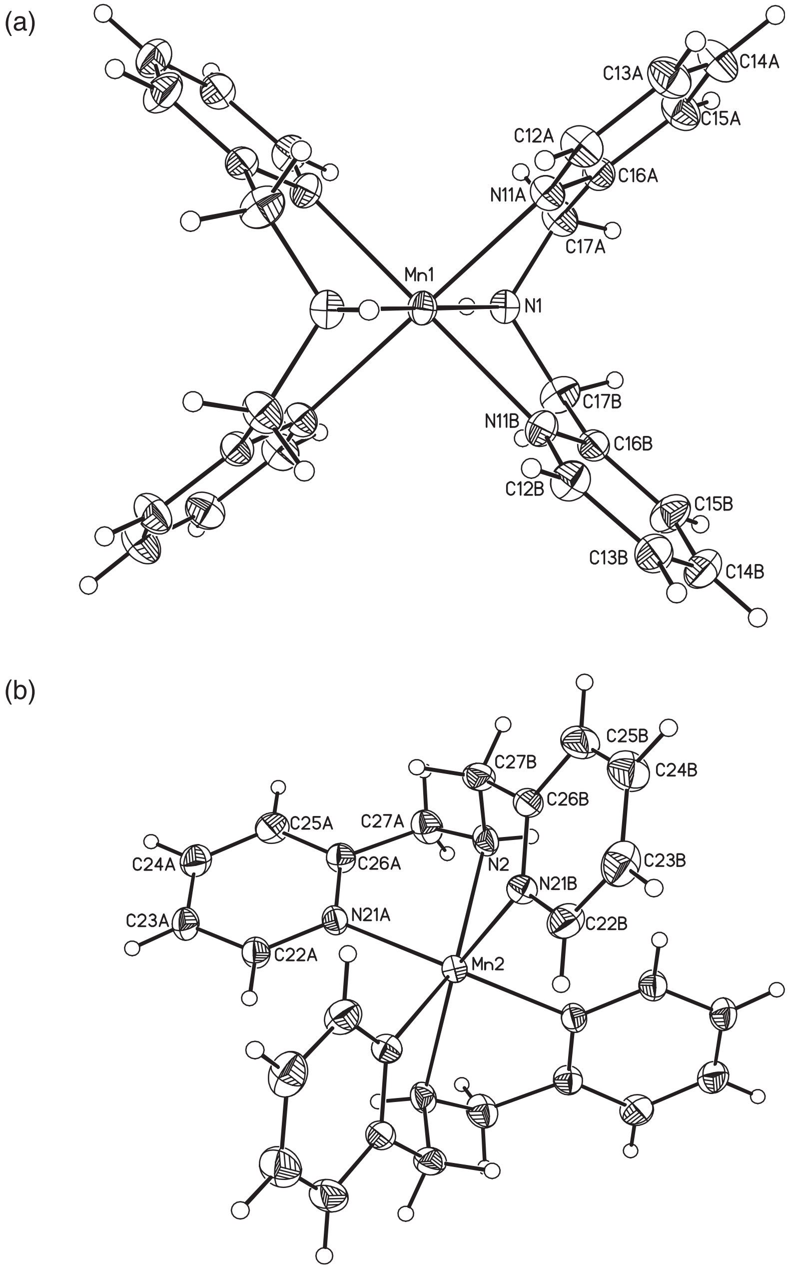

Figure 2. ORTEP drawing of the cations, $[Mn(bpa)_2]^{2+}$, in **1** with C_i (a) and C_2 (b) symmetry. In the C_i isomer the interligand trans angles (Namine–Mn–Namine, Npyridyl–Mn–Npyridyl) are all 180° while in the C_2 isomer, the interligand Namine–Mn–Namine (133.7(2)°), Npyridyl–Mn–Npyridyl (132.8(2)°, and 86.8(2)° are all less than 180°).

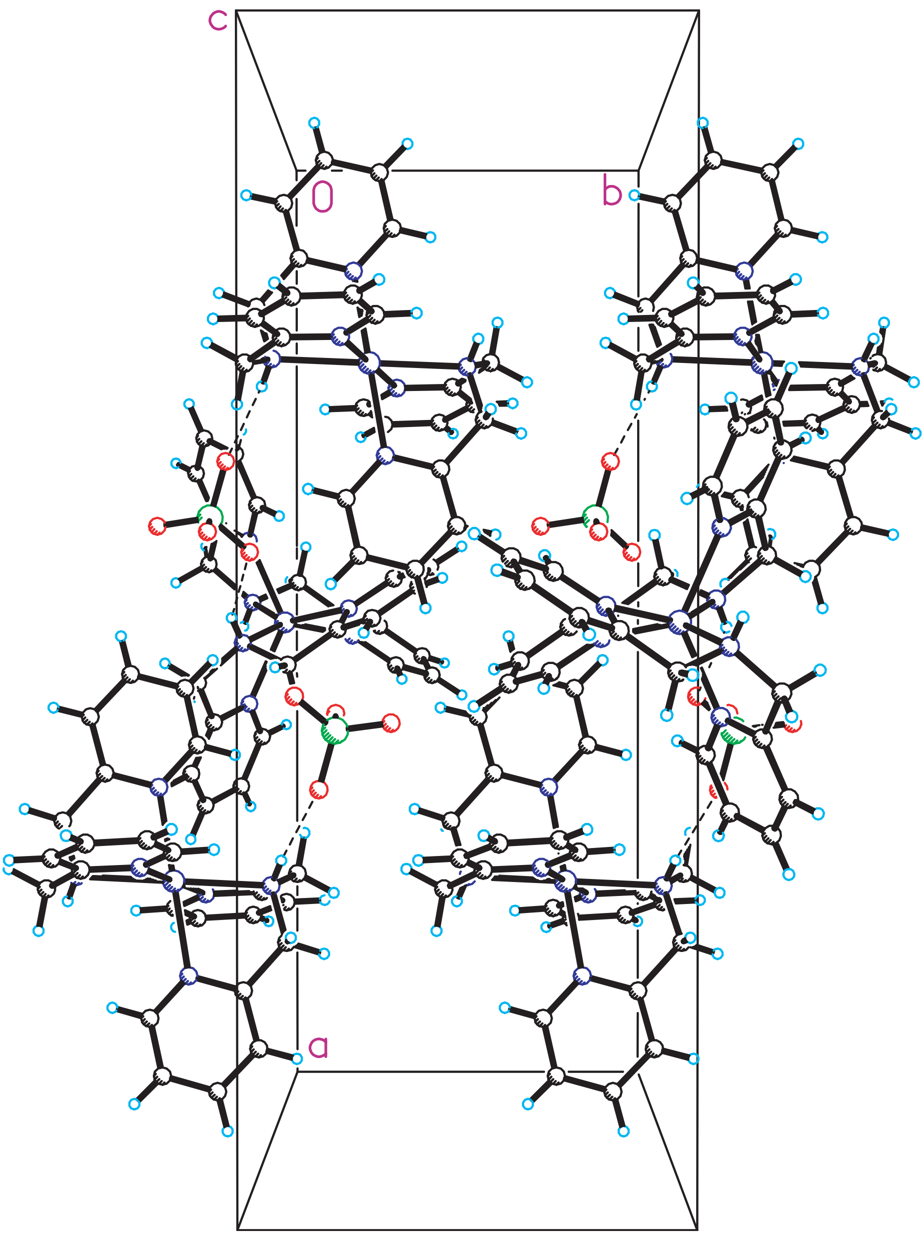

Figure 3. Unit cell packing in the crystals of **1**.

between the bond lengths observed in the two crystalline forms of $[Mn(bpa)_2]^{2+}$ have been reported [1].

Figure 3 shows the unit cell packing in complex **1**. The cations with two different symmetries have alternating arrangement with face-to-face layered stacking of the pyridyl rings of the C_2 cations and edge-to-edge parallel stacking of the pyridyl rings of the C_i cations. These orientations are suggestive of π–π interactions between the pyridyl

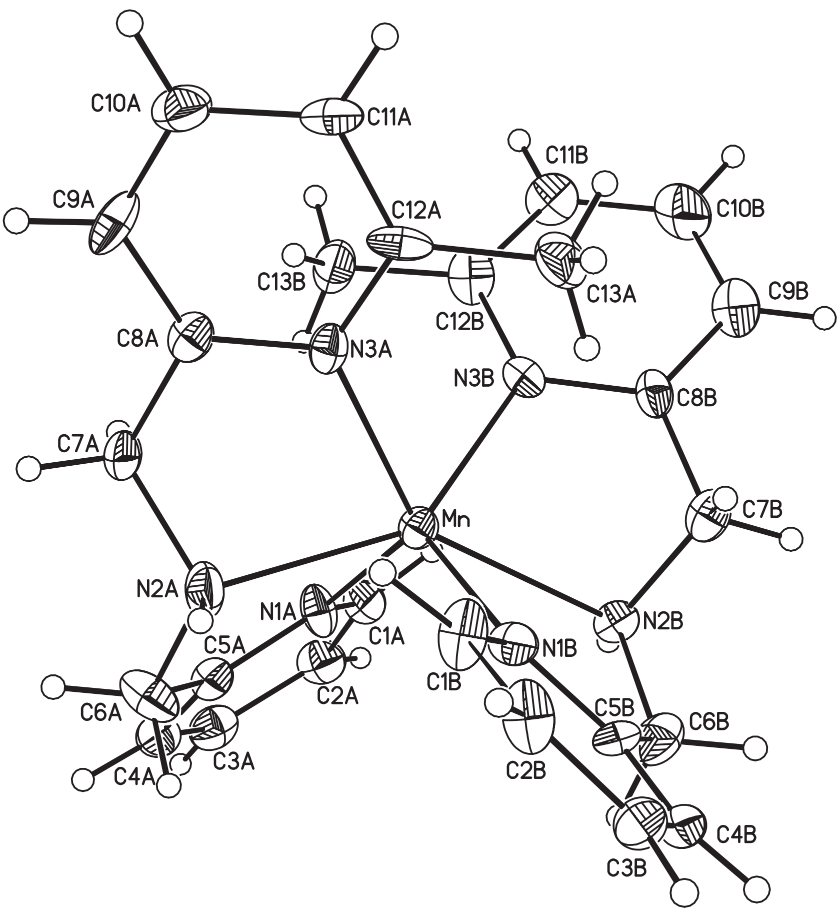

Figure 4. ORTEP drawing of the structure of the cation of **2**, $[Mn(Mebpa)_2]^{2+}$. The interligand N_{amine}–Mn–N_{amine} (N2A–Mn–N2B) bond angle is 139.6(4)° while the interligand $N_{pyridyl}$–Mn–$N_{pyridyl}$ angles are 129.3(4)° and 93.6(5)°.

aromatic rings. The perchlorate oxygens are hydrogen bonded to the amine nitrogens forming a bridge between neighboring C_2 and C_i cations.

3.1.2. Structure of $[Mn(6\text{-}Me\text{-}bpa)_2](ClO_4)_2$ (2). Selected bond lengths and angles (table 3), the ORTEP drawing (figure 4) of the cation of complex **2** and the crystal packing (figure 5) are shown. In the structure of the cation, the Mn(II) coordination has a virtual C_2 symmetry with some distortions resulting in unequal coordination distances of bonds that would be equivalent under the C_2 operation. One of the two ligand molecules in the cation, shows a slightly longer Mn–N_{amine} (by 0.012 Å) and Mn–$N_{pyridyl}$ (by 0.053 Å) bonds than the other, while the second Mn–$N_{pyridyl}$ bond is shorter (by 0.06 Å). The coordination structure in this complex shows some differences from the structure of **1b** in bond angles and bond lengths. Significant among these are that the intraligand $N_{pyridyl}$–Mn–$N_{pyridyl}$ angles (124.7(5)° and 123.8(5)°) in **2** are greater than those of the C_2 isomer of **1** (117.87(12)°); whereas in **2**, the Mn–$N_{pyridyl}$ bond lengths

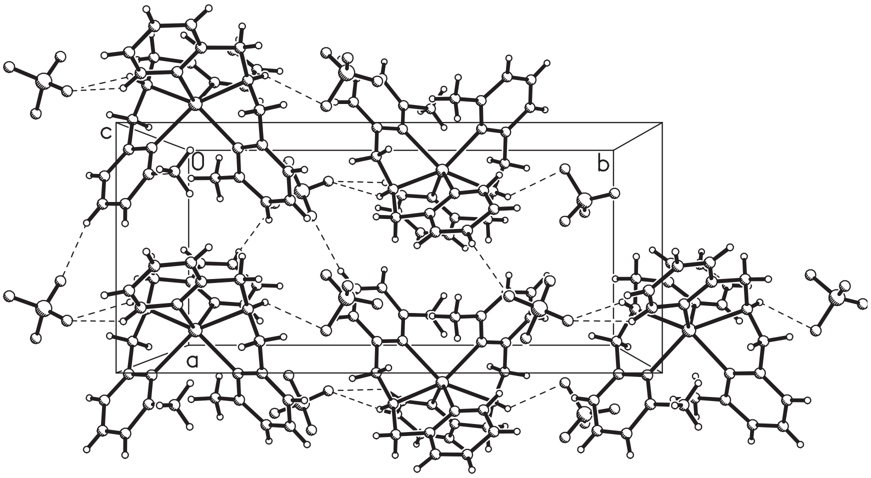

Figure 5. ORTEP drawing of the unit cell packing in crystals of **2**.

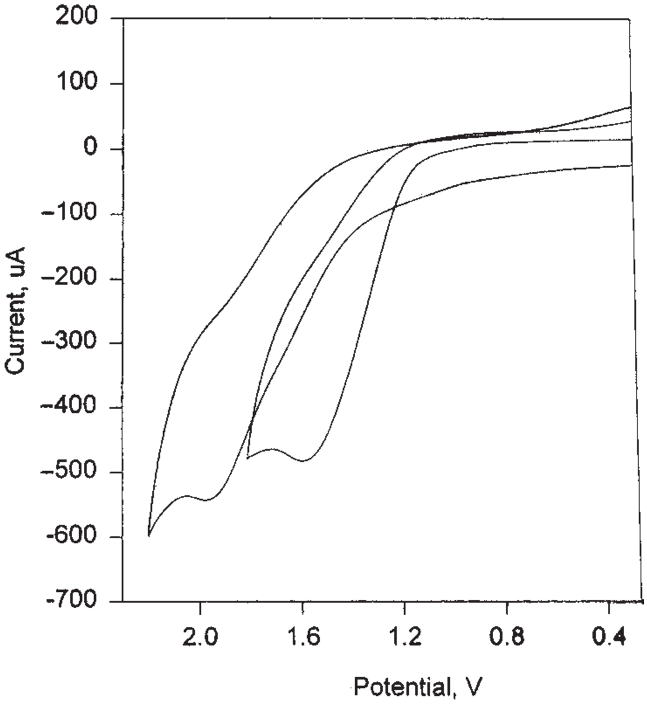

Figure 6. Cyclic voltammograms, in acetonitrile solutions, of **1** and **2** showing the difference in the potentials of the oxidation of the Mn(II) to Mn(III) states.

(which average 2.301(3) Å) are almost the same as those of the Mn–N_{amine} bonds, in **1b**, Mn–$N_{pyridyl}$ bonds (average of 2.235(3) Å) are significantly shorter than the Mn–N_{amine} bonds (by about 0.1 Å). Both of these differences between the two complexes result from the steric effect of the methyl substituent on the pyridyl rings of complex **2**.

The variations in the crystalline forms and coordination geometries of Mn(II) result from the lack of ligand field stabilization energies in high spin d^5 coordination, making steric factors within the molecule and in molecular packing in the crystalline structure predominant in determining the coordination geometry.

The perchlorate ions form hydrogen bonds with the amine nitrogens at distances (longer than 3 Å).

3.1.3. Electrochemistry. Cyclic voltammetric experiments in acetonitrile solution show one irreversible anodic peak for complexes **1** and **2** (figure 6) at 1.60 and 1.90 V, respectively, (*vs.* Ag/AgCl solution) assigned to oxidation of Mn(II) to Mn(III). These are in the normal range for Mn(II)–$N_{pyridyl}$ donor ligand complexes [13, 14]. The substantially higher oxidation potential of complex **2** is attributable to the steric effect of the methyl substituent which increases reorganization energy that goes with the change in oxidation state to Mn(III), which requires coordination rearrangement to regular octahedral geometry and shorter coordination bonds.

3.1.4. Magnetic susceptibility. The room temperature magnetic moments of **1** and **2**, corrected for ligand diamagnetic effects were found to be 5.9, and 6.1 BM, respectively, in the range of values observed for similar Mn(II) complexes.

4. Conclusion

We have studied structural variations in the crystalline state of $[Mn(II)L_2]^{2+}$ where L is bis(2-pyridylmethyl)amine (bpa) or the ring substituted variation 6-Me-bpa, discovering additional examples of C_2 and C_i isomers in the same unit cell of crystals of *facial* Mn(II) *bis* complexes. $[Mn(Me\text{-}bpa)_2]^{2+}(ClO_4^-)_2$ shows only the C_2 isomer and the structure shows the steric effect of the methyl substituent forcing an increase in the Mn–$N_{pyridyl}$ bond lengths which destabilizes the Mn(III) (small radius ion) state relative to the Mn(II) state (relatively larger radius ion) resulting in an increase in the Mn(II)/Mn(III) redox potential of **2** relative to **1**. Higher reorganization energy is needed in oxidation of **2**, due to the additional steric effect of a methyl group substituent ortho to the nitrogen of one of the pyridyl groups of the ligand in complex **2**.

Supplementary material

Crystallographic data (excluding structure factors) have been deposited with Cambridge Crystallographic Data Center as supplementary publications. Copies of the data can be obtained free of charge, on application to CCDC, 12 Union Road, Cambridge CB2 1EZ, UK (Fax: +44 1223 336033 or Email: deposit@ccdc.cam.ac.uk).

Acknowledgements

YG would like to acknowledge the financial support of the NIH through the MBRS program of the Graduate School of Arts and Sciences of Howard University and the

Chemistry Department of Howard University for the support of graduate students. RJB would like to acknowledge the financial support of the DOD in the upgrading of the X-ray diffractometer in the department.

References

[1] J. Glerup, P.A. Goodson, D.K. Hodgson, K. Michelson, K.M. Nielsen, H. Wiehle. *Inorg. Chem.*, **31**, 4611 (1992).

[2] M. Palaniandavar, R.J. Butcher, A.W. Addison. *Inorg. Chem.*, **35**, 467 (1996).

[3] M. Palaniandavar, T. Pandiyan, M. Lakshiminarayanan, H.J. Manohar. *Chem. Soc., Dalton Trans.*, 455 (1995).

[4] R.J. Butcher, A.W. Addison. *Inorg. Chim. Acta*, **158**, 211 (1989).

[5] K.J. Oberhausen, J.F. Richardson, R.M. Buchanan. *Polyhedron*, **8**, 659 (1989).

[6] Y. Gultneh, R.A. Khan, B. Ahvazi, S. Chaudhry, R.J. Butcher. *J. Inorg. Biochem.*, **75**, 7 (1999).

[7] J.K. Romary, J.E. Bund, J.D. Barger. *J. Chem. Eng. Data*, 1229 (1967).

[8] C.B. Storm, C.M. Freeman, R.J. Butcher, A.H. Turner, N.S. Rowan, F.O. Johnson, E. Sinn. *Inorg. Chem.*, **22**, 849 (1983).

[9] J.T. Spencer, M.R. Pourian, R.J. Butcher, E. Sinn, R.N. Grimes. *Organometallics*, **2**, 335 (1987).

[10] G.M. Sheldrick. *SHELXTLPC, Microcomputer Programs for Structure Determination on a PC*, University of Göttingen, Germany (1989).

[11] I. Karle, J. Karle. *Acta Crystallogr.*, **21**, 849 (1966).

[12] International Tables for X-ray Crystallogrpahy, Vol. IV, Kynoch, Birmingham, UK (1974) (Present distributor: Reidel, Dordrecht, The Netherlands).

[13] M.M. Morrison, T.D. Sawyer. *Inorg. Chem.*, **20**, 333 (1989).

[14] Y. Gultneh, A. Farooq, S. Liu, K.D. Karlin, J.A. Zubieta. *Inorg. Chem.*, **31**, 3607 (1992).